American Mineralogist, Volume 88, pages 87–92, 2003

The effect of thermal decarbonation on stable isotope compositions of carbonates

Z.D. SHARP,[1,*] J.J. PAPIKE,[1,2] AND T. DURAKIEWICZ[3,4]

[1]Department of Earth and Planetary Sciences, Northrop Hall, The University of New Mexico, Albuquerque, New Mexico 87131, U.S.A.
[2]Institute of Meteoritics, Earth and Planetary Sciences, University of New Mexico, Albuquerque, New Mexico 87131, U.S.A.
[3]Los Alamos National Laboratory, Condensed Matter & Thermal Physics Group, Mailstop K.764, Los Alamos, New Mexico 87545, U.S.A.
[4]Mass Spectrometry Laboratory, Institute of Physics, Maria Curie-Sklodowska University 20-031 Lublin, Poland

ABSTRACT

Oxygen and C isotope compositions of CO_2 gas released by thermal decomposition of siderite, calcite, and dolomite were measured using a new "real-time" continuous-flow technique to determine whether fractionation associated with simple thermal decarbonation could explain the large isotopic variations and mineralogy such as those found in the ALH84001 meteorite.

Oxygen and C isotope fractionation between calcite or dolomite and evolved CO_2 gas during thermal decarbonation in a 3 bar He pressure environment is very small. The $\delta^{13}C$ and $\delta^{18}O$ values of evolved CO_2 gas are nearly identical to those of the carbonate, very different from the calculated equilibrium $\Delta^{18}O_{calcite\text{-}CO_2}$ value of –4 to –5‰ at 800–900 °C or from previous experimental results of decarbonation in vacuum. The kinetic $\Delta^{18}O_{siderite\text{-}CO_2}$ values are ~–2‰, whereas $\Delta^{13}C_{siderite\text{-}CO_2}$ values increase logarithmically with time, from ~1‰ for the earliest stages of decarbonation to >5‰ in the final stages. Incomplete siderite decomposition produces both magnetite ($\delta^{18}O$ = 3.5‰ SMOW) and minor graphite. CO and O_2 were detected during the decarbonation process. The data can be explained by simultaneous oxidation and reduction by the reaction:

$$6FeCO_3 \rightarrow 2Fe_3O_4 + 2x\ CO + 4y\ CO_2 + (6 - 2x - 4y)\ C + (5 - x - 4y)\ O_2,$$

where x and y are between 0 and 1. Siderite decomposition in the presence of H_2 gas produces wüstite and Fe metal in place of oxidized Fe minerals.

The experiments in this study are not a perfect analog for possible decarbonation conditions that might have occurred to the carbonates in ALH84001. Nevertheless, the large $\delta^{13}C$ and $\delta^{18}O$ variations observed in ALH84001 (>10‰ for O) are significantly larger than those expected by thermal decarbonation, suggesting instead a low-temperature mechanism for their formation.

INTRODUCTION

The most compelling evidence of fossil biogenic activity from Martian meteorites comes from the chemistry and mineralogy of carbonate globules. Heterogeneous major-element and stable-isotope chemistry of carbonates, and the observation of filamentous magnetite inclusions, are reasonable expressions of biogenic crystallization (Romanek et al. 1994; McKay et al. 1996; Valley et al. 1997; Thomas-Keprta et al. 2000). However non-biogenic mechanisms also have been proposed for the morphology of the magnetite needles and carbonate globules (e.g., Brearley 1998; Golden et al. 2001). In the abiogenic theories of formation, variations in the isotopic composition of formation waters or brines, with shock metamorphic (high P and T) overprints, are proposed to explain the small-scale isotopic variations observed in the carbonates (McSween and Harvey 1999). Another alternative is that high-temperature thermal processes occurred after carbonate formation (Shearer et al. 1999). Thermal decarbonation may result in formation of magnetite inclusions (Brearley 1998) and could produce isotopic zoning, a possibility explored in this paper.

Oxygen isotope fractionations of >4‰ have been measured during decarbonation of calcite at high temperatures (McCrea 1950), and in excess of 6‰ for dolomite decarbonated between 500 and 600 °C (Sharma and Clayton 1965). Isotopic fractionations of this magnitude, coupled with Rayleigh behavior, could result in very large isotopic variations on a small scale. To further explore the effects of thermal decarbonation at higher pressures and in "real time," natural carbonate minerals were heated in a He stream at a pressure 2 bars above atmospheric (3 bars absolute) until decarbonation temperatures were reached. Continuous measurements of $\delta^{13}C$ and $\delta^{18}O$ values were made on the evolved CO_2 gas. This approach allows for both instantaneous and time-integrated isotopic fractionation between carbonate and CO_2 to be measured. The first is a measure of the kinetic or equilibrium fractionation between mineral and gas; the second is a monitor of the mechanism by which gas is released from the sample, either in a batch mode or Rayleigh-like fractionation.

METHODS

Starting materials were large single carbonate crystals. Calcite and dolomite came from marbles of the Dora Maira Massif, Italy. These are high-grade metamorphic carbonates that lack isotopic zoning and are free of fluid inclusions (Sharp 1992). The siderite sample is a single dark-brown crystal of

* E-mail: zsharp@unm.edu

0003-004X/03/0001–87$05.00

unknown origin taken from the University of Lausanne sample collection. It is free of iron oxide and graphite inclusions. Coarse (1–3 mm diameter) crushed fragments were loaded into a long quartz tube (6 mm O.D.), which was then packed with quartz wool to keep the carbonate samples fixed in the hot spot of the furnace. Samples were heated with an external resistance furnace surrounding the quartz tube in a He-stream at 2 bars above atmospheric pressure. Temperature was monitored with a digital thermocouple placed adjacent to the tube at the position of the carbonate sample. 250 µL aliquots of the CO_2-bearing He gas were sampled using an automated 6-way switching valve system (Finnigan MAT GasBench II). Simultaneous $\delta^{13}C$ and $\delta^{18}O$ measurements were made of individual aliquots using a Finnigan MAT Delta Plus mass spectrometer. Precision of each measurement was ±0.1‰. Bulk $\delta^{13}C$ and $\delta^{18}O$ values of each carbonate were measured using the conventional phosphoric acid technique (McCrea 1950) at 50 °C using the following fractionation factors: $\alpha_{CO_2\text{-calcite}} = 1.009311$ (Swart et al. 1991), $\alpha_{CO_2\text{-dolomite}} = 1.01066$, and $\alpha_{CO_2\text{-siderite}} = 1.010461$ (Rosenbaum and Sheppard 1986). Carbon isotope data are reported relative to PDB, oxygen to SMOW calibrated to $\delta^{13}C$ and $\delta^{18}O$ values of NBS-19 = 2.02 and 28.85‰, respectively (Hut 1987).

Samples were heated slowly from room temperature, continually monitoring the amount of CO_2 evolved. Analyses were made every 90 seconds by switching the 6 way valve. Reference gas was admitted approximately every 10 minutes to check for mass spectrometer drift. Once a CO_2 signal in excess of several volts (at mass 44) was observed in the mass spectrometer, the temperature was stabilized and kept constant for the remainder of the run. Sample decarbonation continued until signal strength decreased, indicating that the bulk of the carbonate had broken down. The integrated area under each sample peak was used as a measure of the quantity of gas released. The abundance determination is relative, but can be used to determine the amount of CO_2 released at each step relative to the total released during the entire decarbonation experiment. Results are presented in Tables 1–3. Delta values are corrected for the slight drift that occurred over the course of each run, as determined by small (generally less than 0.5‰) drift in the reference gas over the same time interval.

TABLE 1. Isotope data for thermal decomposition of calcite

t (mins after first release)	*T* (°C)	$\delta^{18}O$‰* (SMOW)	$\delta^{13}C$‰* (PDB)	Peak area	% total area	Reaction progress
0	720	16.33	–0.62	0.63	0.15	0.15
1	750	18.79	0.26	2.06	0.95	1.09
3	770	18.82	0.30	5.89	1.36	2.45
4	785	18.71	0.29	14.20	3.28	5.73
5	820	18.80	0.34	28.10	12.96	18.69
7	824	18.79	0.28	32.17	7.42	26.12
8	817	18.73	0.26	25.24	11.65	37.76
10	826	18.59	0.08	25.30	35.01	72.82
16	820	18.15	0.17	15.38	3.55	76.32
17	820	18.22	0.26	16.55	7.64	83.96
19	827	17.87	0.20	16.26	3.75	87.71
20	829	17.70	0.19	14.20	6.55	94.26
22	829	17.06	0.23	9.63	2.22	96.48
23	830	16.55	0.01	5.05	2.33	98.81
25	830	15.86	–0.30	2.14	0.99	99.80
27	830	16.43	–0.02	0.85	0.20	100.00

* Accepted value: $\delta^{13}C$ = 0.33‰ (PDB); $\delta^{18}O$ = 18.44‰ (SMOW).

TABLE 2. Isotope data for thermal decomposition of dolomite

t (mins after first) release)	*T* (°C)	$\delta^{18}O$‰* (SMOW)	$\delta^{13}C$* (PDB)	Peak area	% total area	Reaction progress
0	600	12.55	–2.64	1.12	0.12	0.12
1	630	9.87	–1.91	2.92	0.64	0.77
3	670	9.22	–1.83	12.64	1.40	2.16
4	700	9.04	–2.18	13.00	1.43	3.60
5	698	8.97	–2.57	7.44	1.64	5.24
7	698	8.94	–2.54	6.22	0.69	5.93
8	697	8.82	–2.17	5.80	1.28	7.21
10	697	8.70	–2.44	5.56	0.61	7.82
11	697	9.20	–2.27	5.34	5.30	13.12
20	697	9.20	–2.37	4.06	0.45	13.57
21	697	9.26	–2.22	3.98	0.88	14.45
23	697	9.49	–2.10	3.93	0.43	14.88
24	697	9.63	–2.21	3.91	0.43	15.32
25	697	10.04	–2.39	3.91	0.43	15.75
26	697	9.56	–2.29	3.94	0.87	16.62
28	697	9.78	–2.71	3.96	0.87	17.49
30	697	9.74	–2.45	4.00	0.88	18.37
32	697	9.26	–2.57	4.03	0.89	19.26
34	697	9.29	–2.72	4.07	5.38	24.65
46	730	9.18	–2.75	8.69	1.92	26.56
48	747	9.13	–2.73	13.02	2.87	29.44
50	747	9.02	–2.57	19.04	2.10	31.54
51	764	8.48	–2.38	30.39	6.71	38.25
53	771	8.86	–2.05	45.63	5.04	43.28
54	780	9.15	–1.90	53.09	11.72	55.00
56	780	9.17	–2.01	44.21	4.88	59.88
57	782	9.08	–2.20	28.67	6.33	66.21
59	781	9.09	–2.70	27.25	6.02	72.23
61	781	9.35	–3.11	27.68	27.50	99.72
70	860	8.11	–6.11	2.52	0.28	100.00

* Accepted value: $\delta^{13}C$ = –2.62‰ (PDB); $\delta^{18}O$ = 9.26‰ (SMOW).

TABLE 3. Isotope data for thermal decomposition of siderite

t (mins after first release)	*T* (°C)	$\delta^{18}O$‰* (SMOW)	$\delta^{13}C$* (PDB)	Peak area	% total area	Reaction progress
0	500	20.55	–9.87	11.10	2.61	2.61
2	510	20.66	–9.39	15.97	1.89	4.48
3	520	20.71	–8.79	25.35	5.95	10.43
5	525	20.69	–8.62	30.20	3.55	13.95
6	529	20.95	–8.44	34.28	8.05	22.03
8	529	20.91	–8.49	31.42	7.38	29.41
10	532	21.20	–8.29	28.68	6.73	36.14
12	532	21.25	–8.23	28.63	20.50	56.44
18	527	21.43	–8.04	21.44	5.03	61.48
20	526	21.22	–8.15	19.09	2.24	63.72
21	526	21.09	–8.18	17.06	4.01	67.72
23	526	21.34	–7.93	15.49	1.82	69.54
24	527	21.29	–7.89	14.36	3.37	72.92
26	528	21.18	–7.91	13.39	3.14	76.00
28	528	21.32	–7.93	13.10	1.54	77.60
29	528	21.20	–7.79	12.50	8.61	86.40
35	527	21.02	–7.57	8.70	1.02	87.42
36	527	20.98	–7.66	7.76	2.73	90.16
39	527	21.30	–7.52	6.92	0.81	90.97
40	527	21.12	–7.52	6.13	1.44	92.41
42	527	21.66	–7.19	5.43	1.27	93.68
44	527	21.26	–7.17	4.80	0.56	94.25
45	527	21.42	–7.13	4.25	1.00	95.25
47	526	21.27	–7.13	3.75	2.64	97.89
53	525	21.62	–6.98	2.21	0.32	98.41
55	525	21.32	–6.60	1.90	0.22	98.63
56	525	21.15	–6.86	1.66	0.19	98.83
57	525	20.53	–7.02	1.45	0.17	98.99
58	525	20.64	–6.12	1.27	0.30	99.29
60	525	19.98	–6.46	1.10	0.39	99.68
63	524	21.15	–7.11	0.95	0.22	99.90

* Accepted value: $\delta^{13}C$ = –11.20‰ (PDB); $\delta^{18}O$ = 19.05‰ (SMOW).

Carbon monoxide was monitored in separate runs on splits of the same samples of siderite. Carbon monoxide is present as a product gas, but efforts to determine the $\delta^{13}C$ and $\delta^{18}O$ values were not successful as the measurements were extremely scattered. Oxygen was also scanned for and found in the siderite experiment, but not in others. The $\delta^{18}O$ value of magnetite produced during decarbonation of siderite was measured using the laser fluorination technique (Sharp 1990).

RESULTS

Calcite

Decarbonation of calcite in a He atmosphere began at 720 °C, but the rate significantly increased at 820 °C. After an initial low $\delta^{18}O$ value of 16.4‰ at 720 °C associated with very early decarbonation, $\delta^{18}O$ values increased to a nearly constant 18.7‰, only slightly higher than the accepted value of 18.45‰ (as determined conventionally) for the calcite itself. After 10 minutes at 820 °C, $\delta^{18}O$ values and signal strength both decreased to a final value of 15.7‰, generating very small amounts of CO_2 (Fig. 1). In contrast, $\delta^{13}C$ values were extremely constant (0.12 ± 0.25‰) for all measurements, in good agreement with a value of 0.33‰ determined conventionally.

The $\delta^{18}O$ values of evolved CO_2 gas changed as the reaction proceeded. The degree of reaction progress for each measurement relative to the total was calculated from the cumulative sum of the area under sample peaks 1 to *m* relative to the sum of the sample area of all peaks. Mathematically, this equation is given by

$$\xi = \frac{\sum_{i}^{m} A_i}{\sum_{i}^{M} A_i} \quad (1)$$

where ξ is the reaction progress, A_i is integrated area of sample peak *i*, *m* is the sample number, and *M* is the total number of sample peaks. The $\delta^{18}O$ values decreased smoothly as a function of ξ, consistent with the evolved CO_2 gas having a higher $\delta^{18}O$ value than the calcite (Fig. 2a). The data can be fit by a simple Rayleigh fractionation model, given by:

$$\delta_f = \delta_i + (1000 + \delta_i)[F^{(\alpha-1)} - 1] \quad (2)$$

where $F = 1 - \xi$, α is the fractionation between CO_2 gas and calcite $\left(\text{i.e.,}\alpha_{CO_2-\text{calcite}} = \frac{1000+\delta_{CO_2}}{1000+\delta_{\text{calcite}}}\right)$, δ_i is the initial $\delta^{18}O$ value of the calcite, and δ_f is the delta value for each fraction of ξ. Rearranging Equation 2 in a linear form gives:

$$\log(\delta_f + 1000) = \log(\delta_i + 1000) + (\alpha - 1)\log F \quad (3)$$

A linear regression of the data to Equation 3 gives values for α and δ_i of 1.00054 ± 0.00002 and 18.94 ± 0.04‰, respectively ($R^2 = 0.98$) (Fig. 2b). The α value corresponds to a $\Delta^{18}O_{CO_2\text{-calcite}}$ value of 0.54‰, far less than previous determinations from decarbonation experiments in vacuum (>4‰; McCrea 1950).

Although the O isotope fractionation between CO_2 and calcite is small, the regular changes that can be fit to a Rayleigh fractionation model provide insights into the mechanism by which the carbonate is breaking down. If decarbonation was occurring toward the center of the crystal in a regular "onion skin"-like fashion without any isotopic fractionation with remaining calcite, then the $\delta^{18}O$ values of the evolved CO_2 should

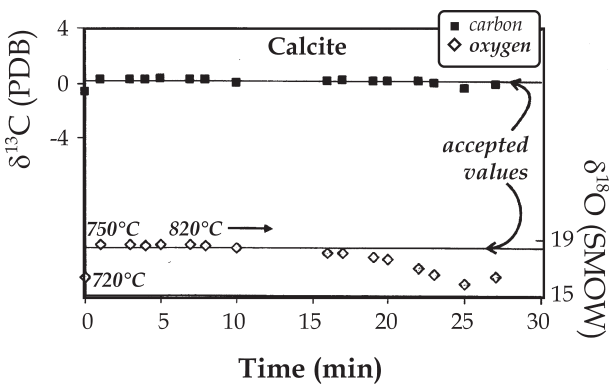

FIGURE 1. Carbon and O isotope compositions of CO_2 gas released during the thermal decomposition of calcite as a function of time. Temperatures are indicated next to data points. Accepted values of carbonates determined using conventional phosphoric acid methods are shown.

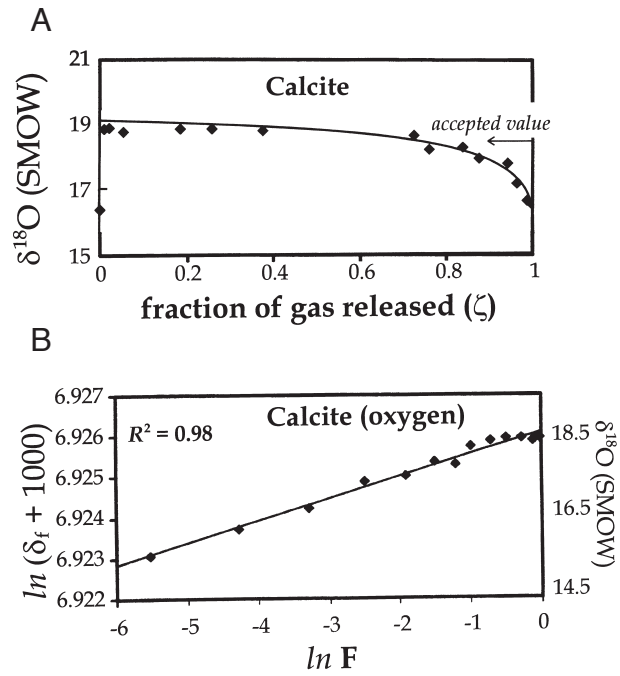

FIGURE 2. (**A**) Oxygen isotope variations as a function of reaction progress. The solid line is a best fit to a Rayleigh fractionation model for removal of oxygen from the sample. (**B**) Linear regression of reaction progress vs. $\delta^{18}O$ value given in the linear form of Equation 3. The straight line fit indicates that these data can be explained mathematically in terms of Rayleigh fractionation.

be constant. They would not necessarily be the same as the carbonate because 1/3 of the oxygen is left behind as CaO. However, there should be no change with time at a constant decarbonation temperature. That the data follow a Rayleigh deearbonation model suggests that the heavy isotopes are preferentially being incorporated into the evolving CO_2 gas, leaving behind residual calcite with ever-decreasing $\delta^{18}O$ values. The $\delta^{18}O$ values of evolved CO_2 in the latter stages of decarbonation are less than those of the total calcite, indicating that the $\delta^{18}O$ values of residual CaO are higher than those of the CO_2 gas. This is reversed from the expected equilibrium fractionation, where the double bond in CO_2 relative to the weak Ca-O bond should result in higher $\delta^{18}O$ values of CO_2 relative to CaO. The consistency of $\delta^{13}C$ with time indicates that there is no isotopic fractionation between calcite and evolved CO_2.

Dolomite

There is much less isotopic variability seen in the course of dolomite decarbonation experiments. CO_2 was first detected at 600 °C. The signal strength increased by an order of magnitude between 670 and 700 °C and again at 760 °C. The first major release of gas at 670–700 °C is probably related to the decarbonation reaction

$$CaMg(C0_3)_2 \rightarrow CaCO_3 + MgO + CO_2 \quad (4)$$

and the second to the decarbonation of the residual calcite (Deer et al. 1978). Both $\delta^{13}C$ and $\delta^{18}O$ values were nearly constant over the entire temperature range and sample size (Fig. 3). There is a small hump in the O data at –18–25% gas released, but this small fluctuation in the δ values does not correspond to any temperature change. The measured $\delta^{18}O$ values average 9.4 ± 0.7‰ (n = 30). For gas released above 700 °C, the average is 9.1 ± 0.2‰ compared with the accepted value determined conventionally of 9.26‰. $\delta^{13}C$ values are similarly constant. The average $\delta^{13}C$ value is –2.50‰ compared with the accepted value of –2.62‰.

Siderite

Siderite decomposition begins at ~450 °C but only begins to generate significant gas at 500 °C. Reaction products identified by X-ray diffraction include magnetite and very minor graphite. SEM imagery of partially decomposed siderite shows patchy areas of siderite in massive magnetite (Fig. 4). Production of CO and O_2 was confirmed with use of the mass spectrometer. Siderite breakdown consists of an auto-oxidation of Fe^{2+} to Fe^{3+} and simultaneous reduction of CO_2 to CO by the reaction (French 1971; Koziol 2000)

$$3\ FeCO_3 \rightarrow Fe_3O_4 + 2\ CO_2 + CO. \quad (5)$$

The presence of graphite requires that either of the additional two reactions occur:

$$CO \rightarrow C + 1/2\ O_2 \quad (6)$$
$$CO_2 \rightarrow C + O_2. \quad (7)$$

giving an overall general reaction of

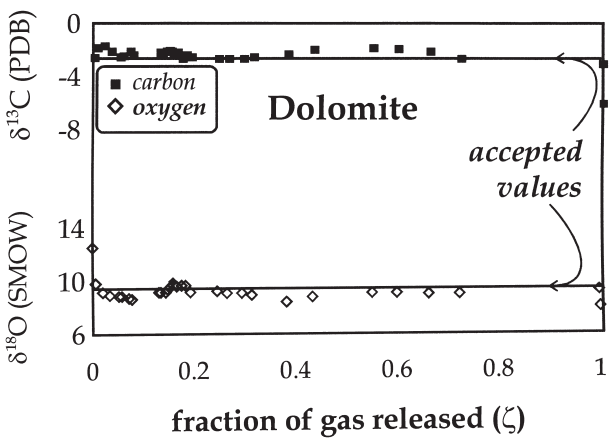

FIGURE 3. Carbon and O isotope compositions of CO_2 gas released during the thermal decomposition of dolomite as a function of total gas released. Accepted values are shown. The delta values are nearly constant for the entire decarbonation experiment and are very close to accepted values for bulk carbonate.

FIGURE 4. SEM image of siderite after partial decarbonation. Patchy areas of siderite remain in an otherwise massive matrix of magnetite. The morphology of the siderite is preserved in the magnetite. (White scale bar = 200 μm).

$$6\ FeCO_3 \rightarrow$$
$$2\ Fe_3O_4 + 2x\ CO + 4y\ CO_2 + (6 - 2x - 4y)\ C + (5 - x - 4y)\ O_2 \quad (8)$$

where x and y vary from 0 to 1.

The $\delta^{13}C$ values of evolved CO_2 gas increase as a function of reaction progress (Figs. 5a and 5b). Linear regression of the data to the Rayleigh fractionation Equation 3 gives a $\delta^{13}C_{initial}$ value of –8.7‰ and a $1000\ln_{CO_2\text{-siderite}} = -0.47 \pm 0.02$‰ ($R^2$ = 0.86). The average $\delta^{13}C$ value of evolved CO_2 (~ –7.7‰) is >3‰ higher than the bulk siderite (–11.2‰). Mass balance for C isotopes is satisfied if the $\delta^{13}C$ value of CO and graphite is less than that of the siderite, offsetting the higher $\delta^{13}C$ values of the evolved CO_2 gas. Production of equal amounts of CO_2 and CO with $\delta^{13}C$ values of –7.7 and –14.7‰, respectively, would equal those of the original siderite. However, the calculated 7‰ fractionation between CO_2 and CO in this study is far less than the equilibrium $\Delta^{13}C_{CO_2\text{-}CO}$ value of ~20‰ at 450 °C (Richet et al. 1977), indicating disequilibrium isotope fractionation during decarbonation. Graphite should have very low $\delta^{13}C$ values, making the mass balance problem even worse.

Initial $\delta^{18}O$ values of evolved CO_2 were ~20.6‰ (SMOW), rising to a relatively stable value of 21.4 ± 0.25‰ (Fig. 5a), higher than the 19.1‰ value of the bulk siderite. The measured $\delta^{18}O$ value of magnetite produced by decarbonation is 3.5‰, and the $\Delta^{18}O_{siderite\text{-}magnetite}$ values of 15.6‰ is larger than the equilibrium value at 500 °C of 8 to 9‰ (Bottinga and Javoy 1975; Carothers et al. 1988; Zheng and Simon 1991), indicating clear disequilibrium. Nearly half of the O from siderite breakdown is incorporated in magnetite, with most of the remainder going to CO_2 (Reactions 5 and 8). The only way to satisfy mass-balance constraints is to produce O_2 gas with a very high $\delta^{18}O$ value (35 to 40‰ SMOW) in molar quantities nearly equal to that of CO_2.

Attempts were made to repeat the siderite decomposition experiment using H_2 as a carrier gas in place of He to evaluate the effect of f_{O_2}. Unfortunately, H_2 apparently combines with CO_2 in the source creating molecular fragments that interfere at mass 45 and especially 46, so that no meaningful $\delta^{13}C$ and $\delta^{18}O$ values could be obtained. The breakdown products of siderite in the presence of the reducing H_2 gas are wüstite and Fe metal. No graphite was detected. Clearly, the oxidation state controls the decarbonation reaction of siderite even in the kinetic decarbonation experiment of this study.

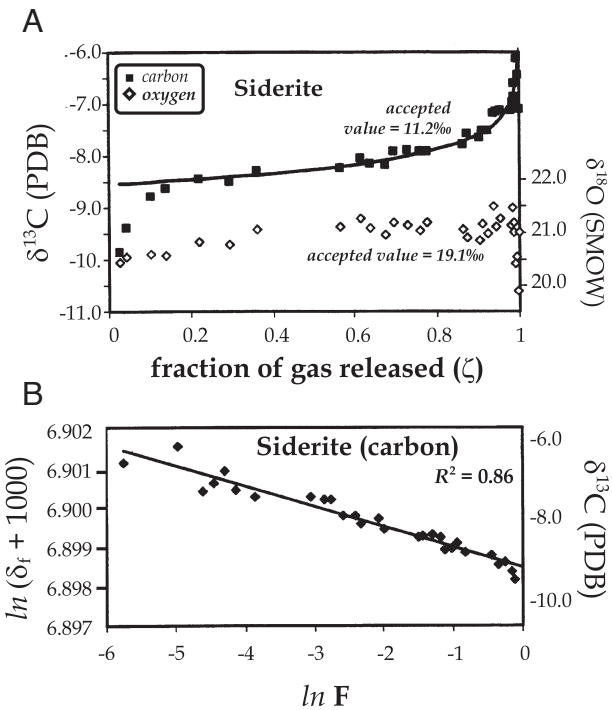

FIGURE 5. (**A**) Carbon isotope variations as a function of reaction progress for decarbonation of siderite. The solid line is a best fit to a Rayleigh fractionation model for removal of carbon from the sample. (**B**) Linear regression of reaction progress vs. $\delta^{13}C$ value given in the linear form of Equation 3. The straight line fit indicates that these data can be explained mathematically in terms of Rayleigh fractionation.

DISCUSSION

Heating and/or shock of a carbonate-bearing material can cause thermal decomposition of the carbonate and simultaneous formation of magnetite as a byproduct (Bradley et al. 1996; Brearley 1998). On the basis of the large isotopic fractionations observed in previous studies performed in vacuum (McCrea 1950; Sharma and Clayton 1965), thermal decarbonation could cause large isotopic heterogeneities in carbonate residues. In the present study, thermal decarbonation experiments were made at higher pressures than in earlier attempts. Although these experiments can mimic the temperature of any naturally occurring thermal decarbonation event, pressures are almost certainly lower. Physiochemical conditions attending decarbonation of samples in nature will be different (e.g., f_{O_2}, f_{H_2O}, etc) from the present experiments as well. Nevertheless, there is a dramatic *decrease* in the fractionation between carbonate and evolved CO_2 gas as pressures are increased from 0 to 3 bars. Rapid decarbonation at high pressures should therefore be too small to explain the dramatic isotopic variations that are seen in ALH84001 (Valley et al. 1997; Leshin et al. 1998).

Under non-vacuum conditions, the $\delta^{13}C$ and $\delta^{18}O$ values of CO_2 gas released during decarbonation of dolomite are nearly identical to those of the bulk carbonate. Overall, the $\delta^{18}O$ value of released CO_2 gas from calcite is the same as the total carbonate, but there is a regular lowering in $\delta^{18}O$ values as the decarbonation reaction proceeds. The data can be fit with a Rayleigh fractionation model, indicating that heavy CO_2 is preferentially released from the crystal. As a result, the $\delta^{18}O$ values become lower during the course of the decarbonation reaction.

The non-equilibrium $\Delta^{13}C_{CO_2\text{-siderite}}$ value is over 3‰, but this is partially a result of the production of CO in the reactcion. The $\delta^{18}O_{sidenie\text{-}magnetite}$ value of 15.6‰ is far less than the equilibrium value of >35‰ at 25 °C. None of the products of any of the decarbonation reactions in this study appear to be in isotopic equilibrium. Thermal decarbonation is a strongly disequilibrium process, but the isotopic fractionations between carbonate and CO_2 in all of the carbonates analyzed—calcite,

dolomite, and siderite—are too small to have a major effect on the isotopic composition of the remaining carbonate. There is almost no fractionation between calcite-CO_2 and dolomite-CO_2. The siderite-CO_2 fractionation is larger, but this difference is a result of production of CO and O_2. Other carbonates, such as breunnerite and magnesite, will almost certainly show *less* fractionation than siderite because their lower Fe contents mean that the effect of redox reactions will be less important.

Magnetite needles are found in ALH84001. If magnetite were to have formed as a byproduct of Fe-rich carbonate breakdown, it must have occurred under relatively oxidizing conditions. At the very reducing conditions of H_2 gas, all Fe remains as Fe^{2+} or is reduced further to Fe.

ACKNOWLEDGMENTS

The research was funded in part by a NASA/JSC subcontract to J.J. Papike from a NASA/Astrobiology Grant to the NASA/ Johnson Space Center (Dave McKay, Principal Investigator). Andrea Koziol is thanked for some exciting ideas concerning the stability of siderite. One of the authors (T.D.) was supported by the Foundation for Polish Science, Warsaw, Poland. Thanks to T. Labotka for his helpful review and D. Cole for his editorial assistance.

REFERENCES CITED

Bottinga, Y. and Javoy, M. (1975) Oxygen isotope partitioning among the minerals in igneous and metamorphic rocks. Reviews of Geophysics and Space Physics, 13, 401–418.

Bradley, J.P., Harvey, R.P., and McSween, H.Y. Jr. (1996) Magnetite whiskers and platelets in the ALH84001 Martian meteorite; evidence of vapor phase growth. Geochimica et Cosmochimica Acta, 60, 5149–5155.

Brearley, A.J. (1998) Magnetite in ALH84001; product of the decomposition of ferroan carbonate. Lunar and Planetary Science Conference, 29.

Carothers, W.W., Adami, L.H., and Rosenbauer, R.J. (1988) Experimental oxygen isotope fractionation between siderite-water and phosphoric acid liberated CO_2 siderite. Geochimica et Cosmochimica Acta, 52, 2445–2450.

Deer, W.A., Howie, R.A., and Zussman, J. (1978) An Introduction to the Rock-Forming Minerals. 528 p. Longman Group Limited, London.

French, B.M. (1971) Stability relations of siderite ($FeCO_3$) in the system Fe-C-0. American Journal of Science, 271, 37–78.

Golden, D.C., Ming, D.W., Schwandt, C.S., Lauer, J., H.V., Socki, R.A., Morris, R.V., Lofgren, G.E., and McKay, G.A. (2001) A simple inorganic process for formation of carbonates, magnetite, and sulfides in Martian meteorite ALH84001. American Mineralogist, 86, 370–375.

Hut, G. (1987) Consultants' group meeting on stable isotope reference samples for geochemical and hydrological investigations. International Atomic Energy Agency, Vienna.

Koziol, A.M. (2000) Carbonate and magnetite parageneses as monitors of carbon dioxide and oxygen fugacity. Lunar and Planetary Science, XXXI.

Leshin, L.A., McKeegan, K.D., Carpenter, P.K., and Harvey, R.P. (1998) Oxygen isotopic constraints on the genesis of carbonates from Martian meteorite ALH84001. Geochimica et Cosmochimica Acta, 62, 3–13.

McCrea, J.M. (1950) On the isotopic chemistry of carbonates and a paleotemperature scale. Journal of Chemical Physics, 18, 849–857.

McKay, D.S., Gibson, E.K., Jr., Thomas-Keprta, K.L., Vali, H., Romanek, C.S., Clemett, S.J., Chillier, X.D.F., Maechling, C.R., and Zare, R.N. (1996) Search for past life on Mars; possible relic biogenic activity in Martian meteorite ALH84001. Science, 273, 924–930.

McSween, H.Y. Jr., and Harvey, R.P. (1999) An evaporation model for formation of carbonates in the ALH84001 Martian meteorite. In G.A. Snyder, C.R. Neal, and W.G. Ernst, Eds., Planetary petrology and geochemistry; the Lawrence A. Taylor 60th birthday volume, p. 252–261. Bellwether Publishing, Columbia.

Richet, P., Bottinga, Y., and Javoy, M. (1977) A review of hydrogen, carbon, nitrogen, oxygen, sulphur, and chlorine stable isotope fractionation among gaseous molecules. Annual Review of Earth and Planetary Science, 5, 65–110.

Romanek, C.S., Grady, M.M., Wright, I.P., Mittlefehldt, D.W., Socki, R.A., Pillinger, C.T., and Gibson Jr., E.K. (1994) Record of fluid-rock interactions on Mars from the meteorite ALH84001. Nature, 372, 655–657.

Rosenbaum, J. and Sheppard, S.M.F. (1986) An isotopic study ofsiderites, dolomites and ankerites at high temperatures. Geochimica et Cosmochimica Acta, 50, 1147–1150.

Sharma, T. and Clayton, R.N. (1965) Measurement of 0-18/0-16 ratios of total oxygen of carbonates. Geochimica et Cosmochimica Acta, 29, 1347–1353.

Sharp, Z.D. (1990) A laser-based microanalytical method for the *in situ* determination of oxygen isotope ratios of silicates and oxides. Geochimica et Cosmochimica Acta, 54,1353–1357.

———(1992) In situ laser microprobe techniques for stable isotope analysis. Chemical Geology, 101, 3–19.

Shearer, C.K., Leshin, L.A., and Adcock, C.T. (1999) Olivine in Martian Meteorite Allan Hills 84001; evidence for a high-temperature origin and implications for signs of life. Meteoritics & Planetary Science, 34, 331–339.

Swart, P.K., Burns, S.J., and Leder, J.J. (1991) Fractionation of the stable isotopes of oxygen and carbon in carbon dioxide during the reaction of calcite with phosphoric acid as a function of temperature and technique. Chemical Geology, 86, 89–96.

Thomas-Keprta, K.L., Bazylinski, D.A., Kirschvink, J.L., Clemett, S.J., McKay, D.S., Wentworth, S.J., Vali, H., Gibson, E.K.J., and Romanek, C.S. (2000) Elongated prismatic magnetite crystals in ALH84001 carbonate globules: Potential Martian magnetofossils. Geochimica et Cosmochimica Acta, 64, 4049–4081.

Valley, J.W., Eiler, J.M., Graham, C.M.. Gibson, E.K.J., Romanek, C.S., and Stolper, E.M. (1997) Low-temperature carbonate concretions in the martian meteorite, ALH84001: Evidence from stable isotopes and mineralogy. Science, 275, 1633–1638.

Zheng, Y.F. and Simon, K. (1991) Oxygen isotope fractionation in hematite and magnetite: A theoretical calculation and application to geothermometry of metamorphic iron-formations. European Journal of Mineralogy, 3, 877–886.

MANUSCRIPT RECEIVED SEPTEMBER 11, 2001
MANUSCRIPT ACCEPTED SEPTEMBER 9, 2002
MANUSCRIPT HANDLED BY DAVID R. COLE